Ensemble Models for Identification of Nonlinear Systems with Stick-Slip

Ingrid Pires*, Helon Vicente Hultmann Ayala* and Hans Ingo Weber*
**Department of Mechanical Engineering, Pontifical Catholic University, Rio de Janeiro, Brazil*

Summary. The nonlinear interactions between the drilling equipment and the rock formation result in torsional, axial, and lateral oscillations in oil drilling routines. Concerning torsional oscillations, the stick-slip phenomenon is the most severe stage. This kind of self-sustained vibrations compromise the performance of mechanical systems. Accordingly, adequate mathematical models are required to analyze these vibrations. In this work, we study two different ways of combining system identification techniques. We employ time-domain data of an experimental setup to build ensemble models. Then we simulate the system and compare their effectiveness in enhancing the accuracy of model predictions and reproducing the stick-slip phenomenon.

Introduction

The nonlinear interactions between the drilling equipment and the rock formation result in torsional, axial, and lateral oscillations in oil drilling routines. The stick-slip phenomenon is the most severe stage of torsional oscillations. In these drilling processes, the phenomenon of stick-slip is the alternation of two phases: the stick phase, in which the drill bit remains stopped by the resistive torque, and the slip phase, which begins when the stored energy overcomes the resistive torque, and the bit is set in motion.

Stick-slip oscillations compromise the performance of mechanical systems [1], therefore proper mathematical descriptions are required to simulate and analyze the system. Extensive surveys on drill string modeling and dynamics can be found in [2, 3].

A common practice is to model the nonlinear interaction between the drill string and rock as dry friction. Regarding the stick-slip phenomenon, the complexity of the analysis lies in the fact that two different friction mechanisms govern the motion. During the stick phase, the static friction rules the motion, while velocity-dependent kinetic friction governs it during the slip phase [1].

Practical limitations of analytical analysis motivate the application of system identification, which comprises a set of techniques for building data-based models. The author of [4] classifies system identification techniques in white, gray, and black-box. They differ from each other by the amount of prior knowledge employed in the construction of mathematical models.

This paper explores two different methods of building ensemble models for an experimental drill string setup. The ensemble model, in this context, consists of a combination between grey and black-box approaches. The test rig used in this study uses dry friction contact to simulate the nonlinear interactions present in drilling routines. We employ time-domain data to build the ensemble models and compare their effectiveness in enhancing the accuracy of model predictions and reproducing the stick-slip phenomenon. The main contribution of this work is the investigation of the suitability of the ensemble of gray and black-box approaches for the identification of systems with friction-induced vibrations.

Experimental system

The test rig employed in this study is a horizontal apparatus composed of a DC motor connected to two solid discs by a low stiffness shaft. The shaft transmits torque and motion from the DC motor to the discs, which are free to rotate. Figure 1 displays a picture of the experimental setup.

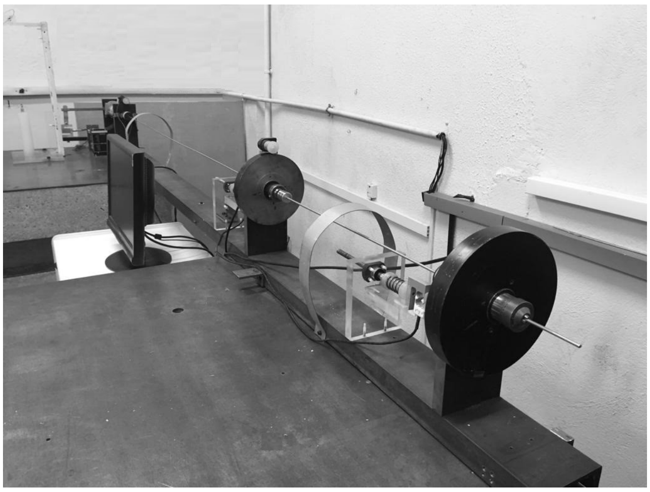

Figure 1: Experimental test rig composed of DC motor, solid discs, and low stiffness shaft.

The rig can replicate the undesired torsional vibrations present in drilling routines. Two braking devices act on the solid

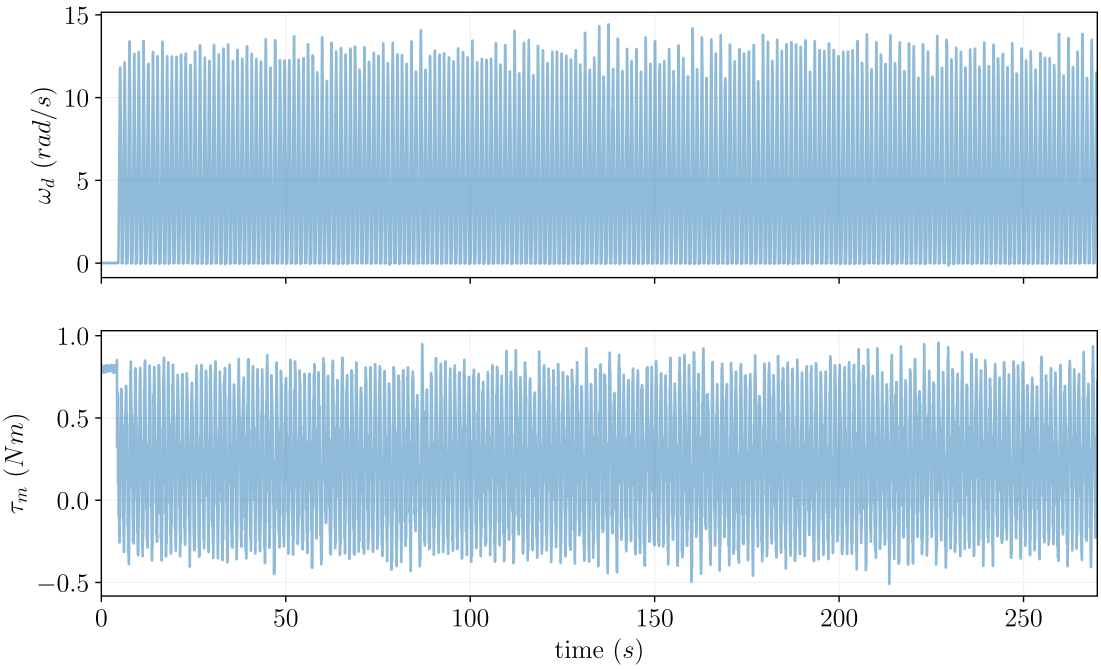

Figure 2: Measured time history of (top) disc angular velocity, ω_d; and (bottom) motor torque, τ_m.

discs to induce friction torque, leading the system to exhibit torsional oscillations and stick-slip. Only the subsystem composed of one of the discs, the intermediary one, and the shaft connecting it to the DC motor is considered in this work.

The dynamical model

Assuming that the subsystem composed of the intermediary disc and the shaft connecting it to the DC motor behaves as a torsional pendulum and that the only resistive torque in the system is caused by the friction torque induced by the braking device, we modeled it as:

$$\begin{aligned} J_d\ddot{\theta}_d + c(\dot{\theta}_d - \dot{\theta}_m) + c_d\dot{\theta}_d + k(\theta_d - \theta_m) &= -T_f, \\ J_m\ddot{\theta}_m + c(\dot{\theta}_m - \dot{\theta}_d) + c_m\dot{\theta}_m + k(\theta_m - \theta_d) &= \tau_m, \end{aligned} \tag{1}$$

where the moments of inertia of the disc and the motor are J_d and J_m. The shaft stiffness is denoted by k and the internal damping by c. c_d and c_m are the external dampings. θ, $\dot{\theta}$, and $\ddot{\theta}$ are the angular displacement, angular velocity, and angular acceleration of the inertias, respectively. The resistive friction torque on disc D2 is denoted by T_f, and the torque transmitted to the mechanical subsystem is denoted by τ_m.

The experimental data

We utilized a LabView-based Data Acquisition System (DAQ) to measure forces, displacements, and velocities. Figure 2 shows the time histories of the disc angular velocity (top) the motor torque (bottom). The motor torque is the system input, and the disc angular velocity is the system output.

We acquired these records for a nominal angular velocity of 5.76 rad/s and an average normal contact force between pin and disc of 50 N. As we can observe in Fig. 2, this combination of nominal angular velocity and normal force leads the system to exhibit stick-slip oscillations. The signals were recorded for 270 seconds.

Methodology

This analysis employs the test rig physical description in two different ensemble models to improve the precision of the predictions. There are three approaches for system identification: white, gray, and black-box. The techniques differ from each other by the amount of prior knowledge used in the mathematical models' construction. The white-box approach applies only physical insight, the gray-box uses less physical information, and the black-box does not involve a priori knowledge. The ensemble models studied in this paper are combinations of gray and black-box components.

This study compares two different methods of building ensemble models. According to [5], one method to build an ensemble model is to use a white-box as a mean function and fit the model residuals using a black-box algorithm. Instead, in this study, we used the gray-box model as a mean function and modeled the residuals with a black-box algorithm:

$$\hat{y_e} = \overbrace{f(x,u)}^{\text{gray-box}} + \overbrace{g(\hat{e},u)}^{\text{black-box}} \tag{2}$$

where $\hat{y_e}$ is the predicted output of the ensemble model. $\hat{y_e}$ is a sum of the predicted system model output $\hat{y_m} = f(x,u)$ and the predicted model residual $\hat{e} = g(\hat{e},u)$. The predicted system output $\hat{y_m}$ is a function of the system input u, and space states x, and the predicted error $\hat{e}$ is a function of the system input u and itself. Another way to construct an ensemble model is to use the information encoded in a white or a gray-box model as an additional input to the black-box. Here, we used the gray-box model output as an input to the black-box as follows:

$$\hat{y_e} = \overbrace{h(e, \underbrace{f(x,u)}_{\text{gray-box}})}^{\text{black-box}} \tag{3}$$

h is a function of the model residual, e, and the output of the gray-box model $f(x,u)$. For simplicity, we name (2) Model 1 and (3) Model 2 in the analysis. Figure 3 gives a general overview of the methodology employed for the formulation of Model 1 and Model 2.

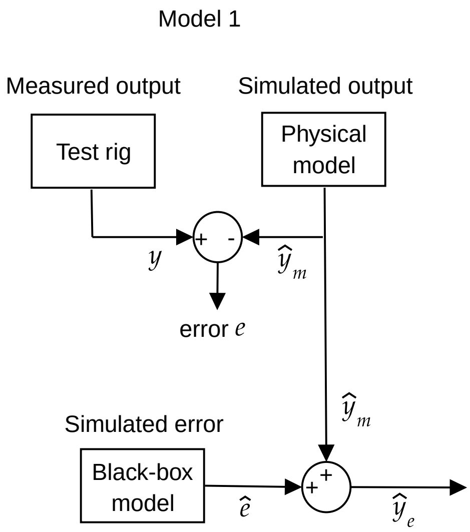

Figure 3: Methodological formulations for (right) Model 1, and (left) Model 2.

Gray-box model

Physical and semi-physical models are particular cases of gray-box models and are related to the estimation of the physical parameters of a system. To estimate the physical parameters of the test rig described by (1), we defined the following state-variables:

$$\mathbf{x} = \begin{bmatrix} \delta & \dot{\theta_d} & \dot{\theta_m} \end{bmatrix}^T,$$

where $\delta = \theta_d - \theta_m$ is the angular difference. Therefore, (1) can be rewritten as a state-space system as follows:

$$\begin{aligned} \dot{\mathbf{x}} &= \begin{bmatrix} 0 & 1 & -1 \\ -k/J_d & -(c+c_d)/J_d & c/J_d \\ k/J_m & c/J_m & -(c+c_m)/J_m \end{bmatrix} \mathbf{x} + \begin{bmatrix} 0 & 0 \\ -1/J_d & 0 \\ 0 & 1/J_m \end{bmatrix} \begin{bmatrix} T_f \\ \tau_m \end{bmatrix} \\ y_m &= \begin{bmatrix} 0 & 1 & 0 \end{bmatrix} \mathbf{x} \end{aligned} \tag{4}$$

where y_m is the output of our gray-box model. The system of (4) is nonlinear since resistive friction torque T_f is a nonlinear function of the disc angular velocity ω_d. T_f is given by:

$$T_f = F_f a, \tag{5}$$

where a is the distance between the disc center and the disc-pin contact point. F_f is the friction force.
The Coulomb friction model states that friction opposes the relative motion between contacting surfaces, and its magnitude is proportional to the normal contact force. The classical Coulomb friction model presents a velocity dependence by the sign function that introduces a discontinuity in the system of ODEs. The regularized Coulomb friction model, instead,

considers the hyperbolic tangent with the transition velocity, v_t, approximation for this study to avoid discontinuities. The following equation defines the regularized model:

$$F_f = F_C \tanh\left(\frac{v}{v_t}\right). \tag{6}$$

where F_f is the friction force, $F_C = \mu_k F_N$ is the magnitude of the Coulomb friction, v is, from the perspective of the body, the relative tangential velocity between the contacting surfaces, F_N is the normal force, and μ_k is the kinetic friction coefficient. For simplicity, we consider $T_C = F_C a$ as the resistive torque related to the kinetic Coulomb friction.

Black-box model

Black-box models are constructed without a priori information. Data acquired from experimentation is used to capture the system dynamics in this modeling. Regarding black-box, we utilized the AutoRegressive eXogenous (ARX) model and the Nonlinear AutoRegressive eXogenous (NARX) model. The ARX structure is:

$$\begin{aligned} y(k) = -(a_1 y(k-1) + a_2 y(k-2) + ... + a_n y(k-n_y)) + \\ (b_1 u(k) + b_2 u(k-1) + ... + b_{n+1} u(k-n_u)), \end{aligned} \tag{7}$$

where $y(k)$, $u(k)$ are the system output and input, respectively; and n_y and n_u are the maximum lags at the system output and input, respectively.

The NARX models are a nonlinear extension of the ARX models [6, 7].The NARX structure is:

$$\begin{aligned} y(k) = F(y(k-1), y(k-2), ..., y(k-n_y), \\ u(k-d), u(k-d-1), ..., u(k-d-n_u)), \end{aligned} \tag{8}$$

F is some nonlinear function, and d is a time delay.

Results and Discussion

We evaluated the performance of the proposed identification methodology via simulation. First, we integrated (4) utilizing the 5th-order Runge-Kutta numerical method with a time step equal to $0,01$ in Matlab. The simulations employed the experimental data for input τ_m. The data set employed for the identification is composed of experimental data from 30 to 90 seconds. And the one used for the validation analyses is composed of experimental data from 120 to 180 seconds.

Table 1 gives the set of estimated parameters obtained employing the system dynamics forward simulation. Using the estimated parameter depicted in Table 1, we simulated the system and calculated the error of prediction to build the ensemble models.

Table 1: Estimated parameters values

k (Nm/rad)	0.1614
c (Ns/m)	0
c_d (Ns/m)	0
c_m (Ns/m)	0.0071
T_C (Nm)	0.2278

For Model 1, the NARX model with motor torque τ_m as input, and error e as output was built as follows:

$$e(k) = \alpha_1 e(k-1) + \alpha_2 e(k-2) + \beta_1 \tau_m(k-1) + beta_2 \tau_m(k-2) +_1 e(k-1)\tau_m(k-1), \tag{9}$$

where α_1, α_2, β_1, β_2, and γ_1 are the parameters of the NARX model. We trained the black-box model with the recorded input and output data of the time interval from 30 to 90 seconds of the recording in Fig. 2 and validated it by employing the recorded input and output data of the time interval from 120 to 180 seconds. We constructed the ensemble model as displayed in (2).

For Model 2, the ARX model with error e and y_m as input, and ensemble model y_e as output was built as follows:

$$y_e(k) = -(a_2 e(k-2) + b_1 y_m(k-1) + b_2 y_m(k-2)) + c_1 y_e(k-1), \tag{10}$$

where a_2, b_1, b_2, and c_1 are the parameters of the ARX model. We trained the black-box model with the recorded input and output data of the time interval from 30 to 90 seconds of the recording in Fig. 2 and validated it by employing the recorded input and output data of the time interval from 120 to 180 seconds. We constructed the ensemble model as displayed in (3).

Figure 4 depicts the free-run prediction obtained with Model 1 (top) and Model 2 (bottom), plotting the direct comparison of experimental and estimated time histories of the disc angular velocity for the validation set. The two ensemble models can reproduce the torsional oscillations with the stick-slip phenomenon observed in the experimental results. Figure 5 shows us one interval of the stick phase, comparing measurements and estimations for the two models.

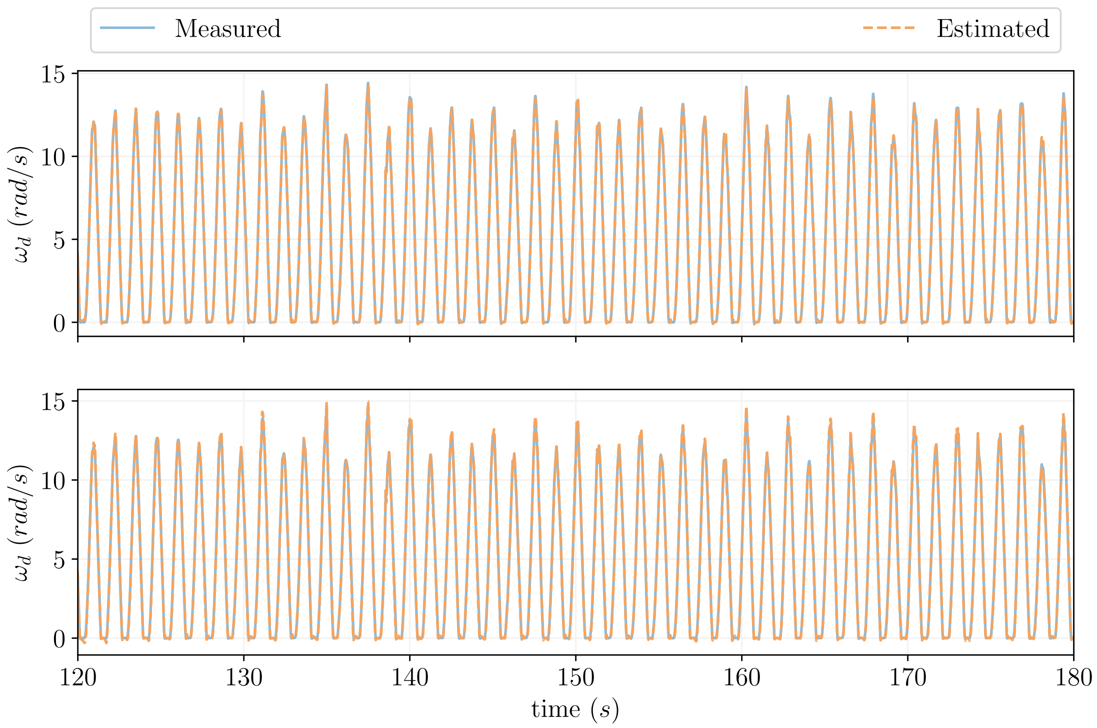

Figure 4: Comparison of measured and predicted disc angular velocity using: (top) Model 1, and (bottom) Model 2.

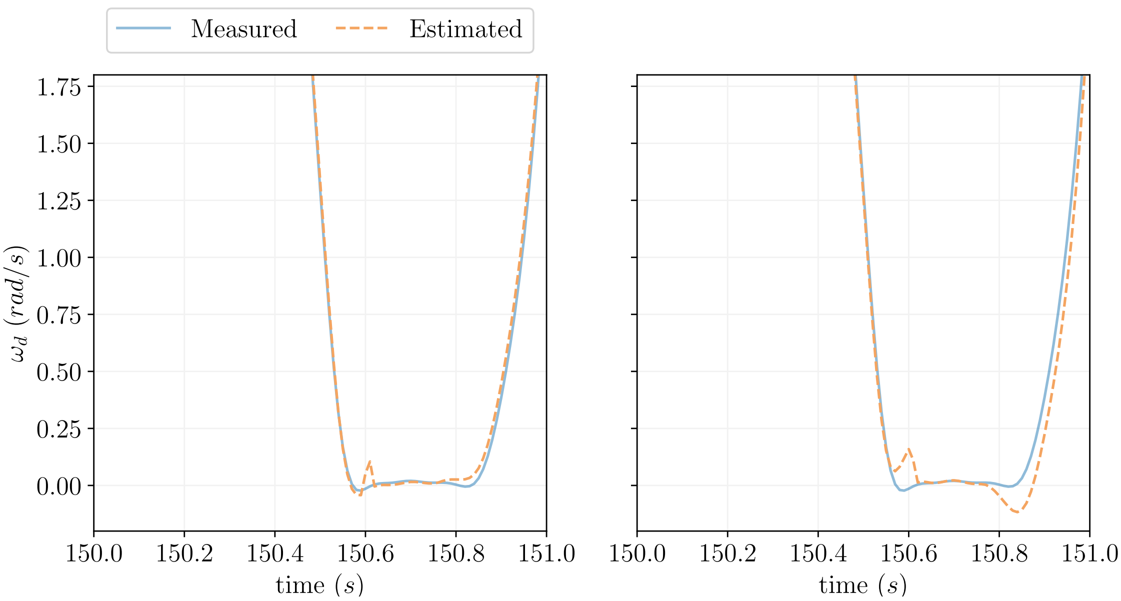

Figure 5: Comparison of measured and predicted disc angular velocity, one stick phase interval, using: (top) Model 1, and (bottom) Model 2.

Figure 6 plots the histogram of the prediction errors for both Models. From the graph of Fig. 6, we can conclude that Model 2 presents the higher prediction errors. Table 2 presents the Root Mean Squared Error (RMSE) and the maximum error for the two ensemble models. From Tab. 2, we see that the ensemble Model 1 presented the lowest RMSE score and the lowest maximum error.

Table 2: RMSE and maximum error scores

	RMSE	max error
Model 1	0.0897	0.3065
Model 2	0.1514	0.4741

As we are interested in the accuracy of predictions and the reproduction of the dynamical phenomenon observed in experimental tests, we also evaluate the average duration of the stick intervals. Table 3 presents the estimated mean stick

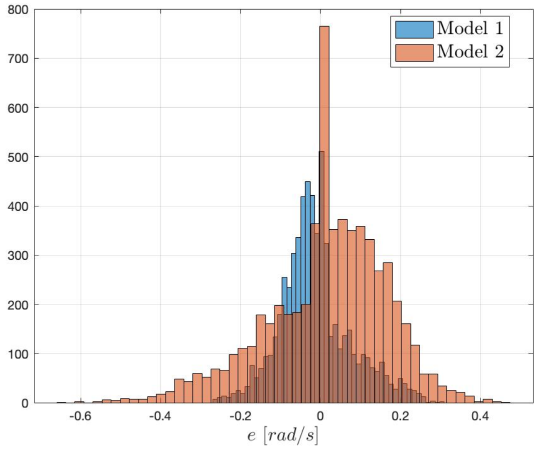

Figure 6: Histogram of prediction errors for Model 1 and Model 2.

duration for the two ensemble models studied. The mean stick interval duration predicted with Model 1, $0.3715s$, is the one that gets closer to the calculated from experimental measurements, that is $0.3770s$.

Table 3: Mean stick duration

Model 1	0.3715
Model 2	0.3913

We chose the RSME, the maximum errors, and the average duration of the stick intervals to compare the model's effectiveness in enhancing the accuracy of predictions and reproducing the stick-slip phenomenon. From the results presented in Table 2 and Table 3, we can say that the ensemble Model 1 performs better in reproducing the test rig experimental data when compared to the ensemble Model 2.

Concluding Remarks

In this work, we compared two different methods of combining system identification techniques. The investigated system is a laboratory test rig that reproduces the torsional vibration of a drill string in drilling operations. We estimated the mechanical parameters and dry contact friction parameters utilizing measured data. With the estimated parameters, we built the ensemble models. Model 1 uses the gray-box model as a mean function and adds the black-box modeled residuals; Model 2 uses the information encoded in the gray-box model as an input to a black-box model.
The proposed ensemble models combine the physics-based approach and ARX or NARX formulations to capture the aspects of the dynamical response missed by the physical model alone. The hybrid formulations were proposed to increase the accuracy of the predictions without losing interpretability.

Acknowledgments

This work has been supported by Brazilian research agencies: CAPES and CNPq.

References

[1] Leine R.I., Van Campen D.H., De Kraker A. (1998) Stick-Slip Vibrations Induced by Alternate Friction Models. *J. Nonlinear Dynamics* **16**:41-54.

[2] Ghasemloonia A., Rideout D.G., Butt S.D. (2015) A review of drillstring vibration modeling and suppression methods. *Journal of Petroleum Science and Engineering* **131**:150-164.

[3] Saldivar B., Mondié S., Niculescu S.I., Mounier H., Boussaada I. (2016) A control oriented guided tour in oilwell drilling vibration modeling. *Annual Reviews in Control* **42**:100-113.

[4] Aguirre L.A. (2015) Introdução à Identificação de Sistemas. editora UFMG, Belo Horizonte, Brazil.

[5] Worden K., Barthorpe R.J., Cross E.J., Dervilis N., Holmes G.R., Manson G., Rogers T.J. (2018) On evolutionary system identification with applications to nonlinear benchmarks. *Mechanical Systems and Signal Processing* **112**:194-232.

[6] Billings S.A., Chen S., Korenberg M.J. (1989) Identification of MIMO non-linear systems using a forward-regression orthogonal estimator. *Journal of Control***6** : 2157-2189.

[7] Aguirre L.A., Billings S.A. (1995) Retrieving dynamical invariants from chaotic data using NARMAX models. *International Journal of Bifurcation and Chaos***2**:449-474.